SARS-CoV-2 Cell Entry Factors ACE2 and TMPRSS2 are Expressed in the Pancreas but Not in Islet Endocrine Cells

Katie C. Coate[1,*], Jeeyeon Cha[1,*], Shristi Shrestha[1], Wenliang Wang[2], Maria Fasolino[2], Ashleigh Morgan[2], Chunhua Dai[1], Diane C. Saunders[1], Radhika Aramandla[1], Regina Jenkins[1], Meghan E. Kapp[3], Roland Stein[4], Klaus H. Kaestner[2], Golnaz Vahedi[2], HPAP consortium[5], Marcela Brissova[1], Alvin C. Powers[1,4,6,7]

[1]Division of Diabetes, Endocrinology and Metabolism, Department of Medicine, Vanderbilt University Medical Center, Nashville, TN, 37232

[2]Department of Genetics and Institute for Diabetes, Obesity, and Metabolism, University of Pennsylvania Perelman School of Medicine, Philadelphia, PA 19104

[3]Department of Pathology, Microbiology and Immunology, Vanderbilt University Medical Center, Nashville, TN, 37232

[4]Department of Molecular Physiology and Biophysics, Vanderbilt University School of Medicine, Nashville, TN, 37232

[5]The Human Pancreas Analysis Program (RRID:SCR_016202)

[6]VA Tennessee Valley Healthcare System, Nashville, TN, 37212

[7]Lead Contact

[*]Co-first authors

Running Title: ACE2 and TMPRSS2 are Not Detected in Pancreatic β cells

Correspondence: al.powers@vumc.org; marcela.brissova@vumc.org

Alvin C. Powers or Marcela Brissova, Vanderbilt University Medical Center, 2215 Garland Ave, Nashville, TN 37232-0475

Summary/Abstract

Reports of new-onset diabetes and diabetic ketoacidosis in individuals with COVID-19 have led to the hypothesis that SARS-CoV-2, the virus that causes COVID-19, is directly cytotoxic to pancreatic islet β cells. This model would require binding and entry of SARS-CoV-2 into host cells via cell surface co-expression of ACE2 and TMPRSS2, the putative receptor and effector protease, respectively. To define ACE2 and TMPRSS2 expression in the human pancreas, we examined six transcriptional datasets from primary human islet cells and assessed protein expression by immunofluorescence in pancreata from donors with and without diabetes. *ACE2* and *TMPRSS2* transcripts were low or undetectable in pancreatic islet endocrine cells as determined by bulk or single cell RNA sequencing, and neither protein was detected in α or β cells from any of these donors. Instead, ACE2 protein was expressed in the islet and exocrine tissue microvasculature and also found in a subset of pancreatic ducts, whereas TMPRSS2 protein was restricted to ductal cells. The absence of ACE2 and TMPRSS2 co-expression in islet endocrine cells makes it unlikely that SARS-CoV-2 directly affects pancreatic islet β cells.

Introduction

In coronavirus disease of 2019 (COVID-19), elevated plasma glucose levels and diabetes have been identified as independent risk factors of morbidity and mortality with severe acute respiratory syndrome-associated coronavirus-2 (SARS-CoV-2) infection (Cariou et al., 2020; Riddle et al., 2020; Wang, 2020; Zhu et al., 2020). Isolated cases of new-onset diabetes and diabetic emergencies such as ketoacidosis and hyperosmolar hyperglycemia have been reported with COVID-19 (Chee et al., 2020; Goldman et al., 2020; Kim et al., 2020; Li et al., 2020a; Rafique and Ahmed, 2020), leading to the hypothesis that SARS-CoV-2 has a diabetogenic effect mediated by direct cytotoxicity to pancreatic islet β cells.

In vitro studies have shown that SARS-CoV-2 entry into human host cells requires binding to the cell surface receptor angiotensin converting enzyme 2 (ACE2) as well as proteolytic cleavage of the viral spike (S) protein by transmembrane serine protease 2 (TMPRSS2) (Hoffmann et al., 2020; Lan et al., 2020; Shang et al., 2020; Wiersinga et al., 2020). In 2010, Yang and colleagues (Yang et al., 2010) examined autopsy samples from patients infected by SARS-CoV-1, which uses similar machinery for binding and cellular entry, and reported expression of ACE2 in pancreatic islet cells from a single deceased donor. Though the identity of these islet cells was not assessed, the authors suggested that binding of ACE2 by SARS-CoV-1 damages islets and causes acute diabetes, which could be reversed after viral recovery (Yang et al., 2010). There have been occasional reports of other viral infections eliciting a diabetogenic effect (reviewed in (Filippi and von Herrath, 2008)). More recently, Yang and colleagues reported that β-like cells derived from human pluripotent stem cells (hPSCs) as well as β-cells of primary human islets express ACE2, raising the possibility of direct infection and cytotoxicity of β cells by SARS-CoV-2 (Yang et al., 2020). Importantly, neither of these prior studies (Yang et al., 2010; Yang et al., 2020) characterized the expression of TMPRSS2, an obligate co-factor for SARS-CoV-2 cellular entry. Thus, a more detailed analysis of both ACE2

and TMPRSS2 expression and localization in human pancreatic tissue from normal donors and those with diabetes is urgently needed. The purpose of this study was to test the hypothesis that pancreatic islet β cells possess the cellular machinery that could render them direct targets of SARS-CoV-2. Importantly, we found that ACE2 and TMPRSS2 are not detectable in human islet endocrine cells from normal donors or those with diabetes, making a direct diabetogenic effect of SARS-CoV-2 unlikely.

Results and Discussion

ACE2 and *TMPRSS2* mRNA expression is minimal in human α or β cells.

We first evaluated mRNA expression of *ACE2* and *TMPRSS2* in FACS-sorted human islet α and β cells from two existing bulk RNA-sequencing (RNA-seq) datasets (Arda et al., 2016; Blodgett et al., 2015) and compared their expression to that of key islet-enriched genes, most of which are normally expressed at relatively low levels in islet cells (e.g., transcription factors). Median expression level of *ACE2* and *TMPRSS*2 mRNA was much less than transcripts of such key islet-enriched genes in human α and β cells (~84% and 92% lower than α and β cell-enriched transcripts, respectively, for DNA-binding transcription factors) (**Figure 1A;** n=7-8 adult donors per study). In addition, analysis of four single-cell (sc) RNA-seq datasets of human pancreatic islets (Baron et al., 2016; Camunas-Soler et al., 2020; Kaestner et al., 2019; Segerstolpe et al., 2016) revealed that *ACE2* and *TMPRSS2* transcripts were either undetectable or minimally expressed in all endocrine subsets (**Figure 1B** and **S3J**). We note that this includes analysis of the robust Human Pancreas Analysis Program (HPAP) dataset that includes more than 25,000 cells (Kaestner et al., 2019) from 11 normal donors and is confirmed by the analysis of three previously reported, but smaller, datasets (**Figure 1B** and **S3J**). Notably, less than 1% of β cells across all four scRNA-seq datasets expressed *ACE2* or *TMPRSS2*.

As for non-endocrine cells, the HPAP dataset (Kaestner et al., 2019) revealed that a small subset (< 5%) of endothelial and stellate cells (which include pericytes) expressed moderate to high levels of *ACE2*, whereas only ~1-3% of either population expressed *ACE2* in the datasets by Baron et al. (Baron et al., 2016) and Segerstolpe et al. (Segerstolpe et al., 2016) (**Figure 1B**). This difference most likely stems from the number of cells analyzed in that the HPAP dataset contains ~2.5- and 20-fold more cells than that of Baron et al. (Baron et al., 2016) or Segerstolpe et al. (Segerstolpe et al., 2016), respectively. In addition, pooled analysis of the

HPAP (Kaestner et al., 2019), Baron et al. (Baron et al., 2016), and Camunas-Soler et al. (Camunas-Soler et al., 2020) datasets showed that less than 1% of acinar or ductal cells expressed *ACE2*, whereas ~35% of both cell types expressed *TMPRSS2*. In the dataset by Segerstolpe et al. (Segerstolpe et al., 2016), *ACE2* was expressed in ~20% of acinar and ductal cells, whereas *TMPRSS2* was expressed in greater than 75% of both populations (**Figure 1B**).

Given that *ACE2* and *TMPRSS2* co-expression is required for SARS-CoV-2 host cell entry (Hoffmann et al., 2020), we evaluated this occurrence and found that on average, less than 1% of acinar, ductal, endothelial and stellate cells co-expressed both transcripts in the HPAP (Kaestner et al., 2019), Baron et al. (Baron et al., 2016) and Camunas-Soler et al. (Camunas-Soler et al., 2020) datasets. In the Segerstolpe et al. dataset (Segerstolpe et al., 2016), ~5% of acinar cells and 15% of ductal cells co-expressed *ACE2* and *TMPRSS2*. Notably, no islet endocrine cells co-expressed *ACE2* and *TMPRSS2* in any of these four datasets. Altogether, these findings greatly reduce the likelihood that SARS-CoV2 can bind and enter human β cells and have direct cytotoxicity.

ACE2 and TMPRSS2 protein are not detected in adult or juvenile human islet α or β cells. Recently, Yang and colleagues (Yang et al., 2020) reported that ACE2 protein was present in α and β cells from primary human islets and in β-like cells derived from hPSCs. To investigate these possibilities, we assessed ACE2 expression by immunostaining on cryosections of intact isolated human islets using the same ACE2 antibody as used by Yang and colleagues (Yang et al., 2020). In accordance with the transcriptomic data reported above, ACE2 was not detected in insulin-positive β cells or glucagon-positive α cells in our samples; instead, ACE2 signal was prominent in supporting cells such as those of the microvasculature (**Figure 1C, top panels**). Since hPSC-derived β-like cells differentiated *in vitro* are considered “juvenile-like” and not functionally mature β cells (Nair et al., 2019), one possibility is that ACE2 is expressed in less

differentiated cells, or in the cultured, immortalized β cells (EndoCβH1) studied by Fignani et al. (preprint: Fignani, 2020). We investigated such a possibility by staining for ACE2 in pancreatic sections from juvenile human donors (age range 5 days to 5 years) using the same ACE2 antibody as used by Yang et al. (Yang et al., 2020). However, ACE2 was not detected in these juvenile β or α cells (**Figure 1C, bottom panels**), making this possibility less likely.

To further characterize ACE2 and TMPRSS2 protein expression in the native pancreas, we next analyzed human pancreatic tissue sections from normal donors (ND, n=14; age range 18-59 years) and those with type 2 diabetes (T2D, n=12; age range 42-66 years) or type 1 diabetes (T1D, n=11; age range 13-63 years). ACE2 protein did not co-localize with markers of α or β cells but was detected within the distinct islet areas indicative of microvascular structures across all ND (**Figures 2A-C'** and **S2A-D**) as well as those with T2D (**Figures 2G-I'** and **S2I-L)** or T1D (**Figures 2M-O'** and **S2O-R**). We noted similar findings with three additional ACE2-directed antibodies, including the same antibodies and dilutions reported by Yang et al. (Yang et al., 2020) and Fignani et al. (preprint: Fignani, 2020), and one antibody validated by the Human Protein Atlas (HPA) (Hikmet et al., 2020) (**Figure S1**).

TMPRSS2 protein was not detected within islets in ND (**Figures 2D-F'** and **S2E-H)**, T2D (**Figures 2J-L'** and **S2M-N**), or T1D donors (**Figures 2P-R'** and **S2S-V**). The TMPRSS2-positive structures in exocrine tissue resembled intercalated and larger ducts as indicated by the typical organization of their nuclei (**Figures 2F'**, **2L'**, and **2R'**). We did not detect differences in the signal intensity or spatial distribution of ACE2 or TMPRSS2 between ND and T2D tissue (**Figures 2** and **S2**) but labeling for both proteins appeared to be reduced in T1D pancreatic sections. Altogether, these data indicate that the host cell surface proteins required for SARS-CoV-2 entry and infection are not present on islet endocrine cells from normal or diabetic donors.

Recent in silico analyses by Vankadari et al. (Vankadari and Wilce, 2020) and Li et al. (Li et al., 2020b) suggested that human dipeptidyl peptidase 4 (DPP4) may interact with SARS-CoV-2 and facilitate its entry into host cells. Therefore, we examined the distribution of DPP4 in human pancreas and found that it localized to α cells, but not β cells, of ND, T2D and T1D islets (**Figure S3A-I**). This finding is consistent with our analysis of four scRNA-seq datasets showing *DPP4*-enriched α cells (**Figures 1A and S3J**). Given that we did not detect TMPRSS2 within islets, these data suggest that DPP4 is an unlikely mediator of β cell entry by SARS-CoV-2 (Drucker, 2020).

The discrepancy between our data and that of previous studies (Yang et al., 2010) (Yang et al., 2020) (preprint: Fignani, 2020) are likely explained by important differences in experimental approaches and contexts. Yang et al. (Yang et al., 2010) showed ACE2 staining in a single donor islet and did not identify its cellular identity with endocrine markers. Furthermore, the ACE2 antibody used in their study was not reported, which precluded replication of their finding. Fignani et al. (preprint: Fignani, 2020) identified ACE2 protein in presumed islet endocrine cells from seven non-diabetic donors; however, ACE2 was primarily seen in subcellular compartments rather than the expected cell surface location. Colocalization of ACE2 with insulin granules in this study raises the possibility of a staining artifact.

ACE2 is localized to islet and exocrine tissue capillaries

The non-endocrine cell staining pattern of ACE2 in islets prompted us to examine whether ACE2 was expressed in the microvasculature, as described in other organs (Hamming et al., 2004). Indeed, staining of adult and juvenile human pancreatic tissue sections with CD31, an endothelial cell marker, revealed that ACE2 labeling was localized to the perivascular compartment of islet capillaries (**Figures 3A-D', I-L'** and **S4A-H'**). In addition, exocrine tissue capillaries, similar to those in islets, showed perivascular ACE2 labeling (**Figures 4E-H'** and

S4I-P'). As ACE2-positive cells were scarce in T1D pancreatic tissues (**Figures 2M-O'** and **S2O-R**), the presence of ACE2 labeling in the perivascular compartment was relatively rare in both islet (**Figure S4E-H'**) and exocrine tissue (**Figure S4M-P'**). The structure and close relationship between ACE2-positive perivascular cells and CD31-positive endothelial cells in islet and exocrine tissue capillaries suggest that ACE2-positive cells are pericytes enveloping capillary endothelial cells of the vascular tube (Almaca et al., 2018). In addition, we observed ACE2-positive cytoplasmic processes extending along CD31-positive endothelial cells colocalized with the extracellular matrix marker collagen-IV within the vascular basement membrane (**Figures 3D'**, **3H'**, **S4D'**, **S4H'**, **S4L' and S4P'**), a pattern that is consistent with pericyte morphology (Almaca et al., 2018). These data support our scRNA-seq analysis of the HPAP dataset which identified a subset of pericytes, marked by *PDGFRB* and *COL1A1*, that express moderate levels of *ACE2* (**Figure 1B**). In addition, our findings are supportive of recent reports of pericyte-specific vascular expression of ACE2 in brain and heart tissue (Chen et al., 2020; He, 2020). Importantly, the absence of *TMPRSS2* co-expression makes it highly unlikely that islet pericytes are susceptible to direct SARS-CoV-2 infection.

Both ACE2 and TMPRSS2 protein are present in pancreatic ducts but rarely overlap

Our work indicated that TMPRSS2 protein was localized to the apical surface of intercalated and larger ducts in ND (**Figures 2D-F'** and **S2E-H**), T2D (**Figures 2J-L'** and **S2M-N**), and T1D pancreatic tissues (**Figures 2P-R'** and **S2S-V**). To further ascertain ductal expression of TMPRSS2 and determine whether ACE2 was expressed beyond exocrine tissue capillaries, we visualized expression of these two proteins in relationship to cytokeratin-19 protein (KRT19), a ductal cell marker. TMPRSS2, but not ACE2, was expressed by KRT19-positive cells on the apical surface of intercalated and larger ducts throughout the exocrine compartment (**Figure 4A-D'**). Rarely, both ACE2 and TMPRSS2 were found on the apical surface of ductal epithelial cells but appeared to be spatially distinct (**Figure 4E-H'**). These findings support our scRNA-seq

analysis in which *TMPRSS2* was more highly expressed in ductal cells than *ACE2*, but cells positive for both *ACE2* and *TMPRSS2* were scarce. Nevertheless, it is possible that SARS-CoV-2 may target such ductal cells and trigger inflammation in those infrequent ductal areas where both ACE2 and TMPRSS2 reside. Although *TMPRSS2* mRNA was detected in acinar cells by scRNA-seq (**Figure 1B**), TMPRSS2 protein was undetectable by immunofluorescence analysis (**Figure 4**).

While recent case reports of patients with COVID-19 have included mild elevations of amylase and lipase or frank pancreatitis (Karimzadeh et al., 2020; Meireles et al., 2020; Rabice et al., 2020; Wang et al., 2020), the vast majority of patients with COVID-19 have neither elevated pancreatic enzymes nor frank pancreatitis (Ashok et al., 2020; Bonney et al., 2020; Bruno et al., 2020). Because rare cells in the exocrine compartment co-express ACE2 and TMPRSS2, it is possible that SARS-CoV-2 could infect those cells, induce pancreatitis, and consequently impact islet function. We examined pancreatic specimens from individuals infected with SARS-CoV-2. Histologic analysis of pancreatic tissue from seven COVID-19 patients, three of whom had diabetes, did not show signs of pancreatitis (**Figure 4I**). Further evaluation of exocrine inflammation in COVID-19 autopsy samples, particularly in those with new-onset diabetes, will be of interest.

Caveats related to the current study include: 1) while it is possible that ACE2 and TMPRSS2 are not the only means for SARS-CoV-2 entry into host cells, the preponderance of literature strongly suggests this is the case (Hoffmann et al., 2020; Lan et al., 2020; Sanders et al., 2020; Shang et al., 2020); 2) we indirectly assessed the permissiveness of human islet endocrine cells to SARS-CoV-2 by examining the expression of ACE2 and TMPRSS2 in human pancreas, but we did not directly measure binding or viral entry into β cells; and 3) we did not analyze ACE2 and TMPRSS2 expression in pancreatic samples from diabetic patients infected with SARS-CoV-2, so changes in the expression and/or localization of these receptors in the setting of COVID-19 infection cannot be excluded.

In summary, recent reviews, commentaries, and clinical guidelines (Apicella et al., 2020; Bornstein et al., 2020; Goldman et al., 2020; Gupta et al., 2020; Heaney et al., 2020) have highlighted an attractive hypothesis of SARS-CoV-2 direct cytotoxicity to β cells. Here, we addressed the fundamental question of whether SARS CoV-2 cell entry machinery is present in β cells of human pancreatic tissue. By examining pancreatic ACE2 and TMPRSS2 expression in normal donors and in those with diabetes, we found that, **1)** neither protein is detectable in α or β cells; **2)** ACE2 is primarily expressed in the islet and exocrine tissue capillaries, and a subset of ductal cells whereas TMPRSS2 is primarily expressed in ductal cells; **3)** ACE2 and TMPRSS2 protein expression and distribution appear similar in ND and T2D pancreata; and **4)** ACE2 and TMPRSS2 are infrequently co-expressed in pancreatic ducts. Together, these mRNA and protein data do not support the hypothesis that SARS-CoV-2 can bind and infect islet α or β cells and lead to cytotoxicity, causing their demise and eliciting new-onset diabetes. Our results indicate that the impact of SARS-CoV-2 on glucose homeostasis is likely mediated by systemic inflammation or changes in organs such as liver, muscle or adipose tissue. Future studies evaluating the status of ACE2 and TMPRSS2 in these tissues will be of interest.

Acknowledgements

We are especially thankful to organ donors and their families. This research was supported by funding provided by the National Institute of Diabetes and Digestive and Kidney Diseases, the Human Islet Research Network (HIRN; RRID:SCR_014393; https://hirnetwork.org; DK112232, DK123716, U01DK123594, DK104211, DK108120), and by DK106755, DK117147, DK117147-01A1S1, DK112217, DK20593, and the Functional Genomics Core of DK19525. This manuscript used data acquired from and available at the Human Pancreas Analysis Program (HPAP-RRID:SCR_016202) Database (https://hpap.pmacs.upenn.edu), a HIRN consortium. This work was also supported by grants from the Doris Duke Charitable Foundation (DDCF 4043516256), JDRF, The Leona M. and Harry B. Helmsley Charitable Trust, the Department of Veterans Affairs (BX000666). Human pancreatic islets were provided by the NIDDK-funded Integrated Islet Distribution Program at the City of Hope (NIH Grant # 2UC4 DK098085 RRID: SCR_014387; http://iidp.coh.org). Human kidney sections were provided by Dr. Agnes B. Fogo at Vanderbilt University. We thank Amber M. Bradley for technical assistance.

Author Contributions: K.C. J.C., M.B., and A.C.P. designed the experiments. K.C., J.C., M.B., and A.C.P. wrote the manuscript. K.C., J.C., S.S., G.V., W.W., A.M., M.F., A.R., R.J., C.D., D.S., R.S., M.E.K., K.L.H., M.B., and A.C.P. performed experiments or analyzed the data. All authors reviewed and edited the final manuscript. As the lead contact, A.C.P. is responsible for: 1) communication with the journal and co-authors; 2) addressing requests for reagents and resources; and 3) overseeing decisions and disputes related to the manuscript.

Declaration of Interests: The authors declare no conflicts of interests

Figure 1. *ACE2* and *TMPRSS2* Expression is Minimal in Isolated Human Islet α and β Cells. (**A**) Relative expression of *ACE2* and *TMPRSS2* compared with select α (white bars) and β (green bars) cell type-enriched genes in sorted human islet α and β cells from previously published bulk RNA-seq datasets, reported as transcript per million mapped reads (TPM; n=7; (Blodgett et al., 2015)) or reads per kilobase of transcript per million mapped reads (RPKM; n=8; (Arda et al., 2016)). Mean expression values are presented as $\log_2$ (TPM+1) or $\log_2$ (RPKM+1) to account for negative values. Dotted line highlights *ACE2* and *TMPRSS2* expression. (**B**) Dot plots of *ACE2* and *TMPRSS2* expression compared with cell type-enriched genes from three single cell (sc) RNA-seq datasets (Baron et al., 2016; Kaestner et al., 2019; Segerstolpe et al., 2016). Dot size indicates percentage of cells in a given population expressing the gene; dot color represents scaled average expression. (**C**) Representative images showing an isolated islet from an adult human donor (top panels) and a pancreatic section from a juvenile human donor (bottom panels) stained for ACE2 (red; antibody ab15348), insulin (INS; green), glucagon (GCG; white), and DAPI (blue). Dotted yellow line denotes islet area. Scale bar is 50 μm. Human pancreatic donor information is available in Table S1 (1C, donors I1-I3, J1-J5). See also Figure S1.

Figure 2. ACE2 and TMPRSS2 Protein is Not Detected in Human Islet α or β Cells in Adult Pancreas. Immunostaining does not detect SARS-CoV-2 cell entry markers ACE2 (**A**, **G**, **M**; antibody ab15348) or TMPRSS2 (**D**, **J**, **P**), both shown in red, in islet α cells (GCG; blue) or β cells (INS, green) in pancreatic sections from adult donors without diabetes (**A-F'**) or from donors with type 2 (**G-L'**) or type 1 (**M-R'**) diabetes. Dotted yellow lines denote islets. Inset areas are marked by a yellow box in MERGE column with DAPI counterstain. Pancreatic ducts, identified structurally by rosette pattern of DAPI-labeled nuclei (white), are shown within dotted yellow lines in INSET column. Scale bars are 100 μm (**A-R**) and 50 μm (Insets, **C'-R'**). Human

pancreatic donor information is available in Table S1 (**A-C'**, donor N2; **D-F'**, donor N8; **G-I'**, donor 2F; **J-L'**, donor 2L; **M-O'**, donor 1F; **P-R'**, donor 1D). See also Figures S1-S3.

Figure 3. ACE2 Protein is Localized to Islet and Exocrine Capillaries in Adult and Juvenile Human Pancreata. Representative images of endothelial cells (CD31, white) and ACE2-positive perivascular cells (red; antibody ab15348) in the adult islet (**A-D**') and exocrine (**E-H'**) microvasculature, as well as in juvenile human islet (**I-L'**) microvasculature. Yellow arrowheads point to CD31-positive endothelial cells, while magenta arrowheads point to perivascular ACE2-positive cells. ACE2-positive perivascular cells abut the extracellular matrix marker collagen-IV within the vascular basement membrane (collagen-IV [COL4], green; **D, D', H, H'**). Inset areas (**A'-L'**) are marked by yellow boxes in **A-L**. In juvenile human pancreas (**I-L'**), ACE2 is not detected in islet endocrine cells expressing insulin and glucagon (ENDO, green); DAPI (blue). Scale bars are 50 μm (**A-L**) and 10 μm (Insets, **A'-L'**). Human pancreatic donor information is available in Table S1 (**A-H'**, donor N2; **I-L'**: donor J4). See also Figure S4.

Figure 4. Analysis of ACE2 and TMPRSS2 Protein Expression in Pancreatic Ducts and Pancreatic Histology. (**A-D'**) TMPRSS2 (green), but not ACE2 (red; antibody R&D AF933), is expressed by KRT19-positive cells (blue) on the apical surface of intercalated and larger ducts throughout the exocrine compartment. DAPI (white). Yellow arrowheads point to TMPRSS2 on the apical surface of ductal cells (KRT19-positive). Magenta arrowheads point to ACE2-positive non-ductal cells. (**E-H'**) Rarely, both TMPRSS2 (green) and ACE2 (red; antibody R&D AF933) were expressed on the apical surface of ductal epithelial cells (KRT19, blue), but appeared to be spatially distinct. Yellow and white arrowheads point to spatially distinct TMPRSS2 and ACE2 labeling, respectively, localized to the apical surface of larger ducts (KRT19-positive cells). Inset areas (**A'-H'**) are marked by yellow boxes in **A-H**. Scale bars are 50 μm (**A-H**) and 10 μm (**A'-H'**). (**I**), Representative H&E image of human pancreas upon autopsy of decedent

after COVID-19 disease. Red line denotes islet; BV, blood vessel; D, duct. Scale bar in green is 100 μm (n=7 donors). Human pancreatic donor information is available in Table S1 (**A-D'**, donor N8; **E-H'**, donor N9; **I**, COVID-19 donor 1).

STAR METHODS

Resource Availability

Lead contact. Further information and requests for resources and reagents should be directed to and will be fulfilled by the Lead Contact, Alvin C. Powers (al.powers@vumc.org).

Materials Availability. This study did not generate new unique reagents.

Data and Code Availability. All data generated or analyzed during this study are included in this published article or in the data repositories listed in the Key Resources Table. Original/source data for Figure 1A (bulk RNA-seq of FACS sorted human islet α and β cells) is available under NCBI GEO accession numbers GSE67543 (Blodgett et al., 2015) and GSE57973 (Arda et al., 2016). Original/source data for Figure 1B and Figure S3J (single cell RNA-seq of human islets) is available under NCBI GEO accession numbers GSE84133 (Baron et al., 2016), GSE124742 (Camunas-Soler et al., 2020), and ArrayExpress (EBI) accession number E-MTAB-5061 (Segerstolpe et al., 2016). This manuscript used data acquired from the Human Pancreas Analysis Program (HPAP) Database (https://hpap.pmacs.upenn.edu), a Human Islet Research Network consortium.

Experimental Model and Subject Details

Human Subjects. Pancreata and islets from juvenile, adult, T1D and T2D human donors were obtained through partnerships with the International Institute for Advancement of Medicine (IIAM), National Disease Research Interchange (NDRI), Integrated Islet Distribution Program

(IIDP), and local organ procurement organizations. Pancreata from normal donors were processed either for islet isolation (Balamurugan et al., 2003) and/or histological analysis as described previously (described below and in Table S1) (Brissova et al., 2018; Dai et al., 2017). Pancreata from COVID-19 decedents after autopsy were obtained from Vanderbilt University Medical Center (Nashville, TN) and processed for histological analysis as according to standard procedures for clinical diagnostics (VUMC Histology Peloris Processing Protocol). Samples from donors of both sexes were used in our analyses. Donor demographic information is summarized in Table S1. The Vanderbilt University Institutional Review Board does not consider de-identified human pancreatic specimens to be human subject research.

METHOD DETAILS

Human Pancreas Procurement and Preparation of Tissue for Histological Analysis. Pancreata from juvenile, adult, T1D and T2D donors were obtained within 18 hours from cross-clamp and maintained in cold preservation solution on ice until processing, as described previously (Balamurugan et al., 2003; Brissova et al., 2018). Pancreata recovered from seven COVID-19 decedants were obtained from Vanderbilt University Medical Center (Nashville, TN) within 8-27 hours of death. Donor demographic information is summarized in Table S1. Human kidney samples were provided by Dr. Agnes Fogo, Vanderbilt University. The Vanderbilt University Institutional Review Board has declared that studies on de-identified human pancreatic specimens do not quality as human subject research.

Mouse Tissue Preparation for Histological Analysis. Mice were maintained on standard rodent chow under a 12-hour light/dark cycle. Kidney from adult NOD.*Cg-Prkdc*^{scid}*Il2rg*^{tm1Wjl}/ Sz (NSG) mice ages 12 to 18 weeks (Jackson Laboratory) were isolated. Tissue specimens were processed for cryosections as described previously (Brissova et al., 2018).

Immunohistochemical Analysis. Immunohistochemical analysis was performed on 5-µm cryosections (Figure 2A-C', G-I' and M-O'; Figure 3 A-H'; Figure S1:1A-E; S2A-D, I-L and O-R; S3, S4 and S5) or on formalin-fixed paraffin embedded (FFPE) pancreatic sections (Figure 2D-F', J-L' and P-R'; Figure 4; Figure S1:2A-E, 3A-E and 4A-D; S2E-H, M-N and S-V) as described previously (Brissova et al., 2014; Brissova et al., 2018; Wright et al., 2020). FFPE sections were first deparaffinized in xylene and ethanol followed by heat-induced epitope retrieval in a citrate-based antigen unmasking solution, pH 6.0 (see Key Resources Table). Immunofluorescence analysis of isolated islets was performed on 8-µm cryosections of islets embedded in collagen gels as described previously (Brissova et al., 2005; Brissova et al., 2018). Primary antibodies to

all antigens and their working dilutions are listed in the Key Resources Table. The antigens were visualized using appropriate secondary antibodies listed in the Key Resources Table. Digital images were acquired with an Olympus FLUOVIEW FV3000 laser scanning confocal microscope (Olympus Corporation).

H&E Staining

FFPE pancreas tissue sections (5-μm sections, n=7 donors) were processed according to standard procedures for clinical diagnostics (Vanderbilt University Medical Center Histology Peloris Processing Protocols). Slides were stained with hematoxylin & eosin and reviewed by a clinical pathologist at Vanderbilt University Medical Center.

Bulk RNA-seq Data Acquisition. Transcripts Per Million (TPM) and Reads Per Kilobase Per Million (RPKM) normalized counts were extracted from publicly available RNA-seq datasets (Arda et al., 2016; Blodgett et al., 2015). The sources of the datasets are summarized in the Key Resources Table. GraphPad Prism v8 was used to generate plots in Figures 1A.

Single Cell RNA-seq Data Acquisition. Raw gene count matrices were extracted from existing single cell RNA-seq datasets (Baron et al., 2016; Segerstolpe et al., 2016, Camunas-Soler et al., 2020) and from the Human Pancreas Analysis Program (HPAP) Database (https://hpap.pmacs.upenn.edu), a Human Islet Research Network consortium. The sources of the datasets are summarized in the Key Resources Table. Gene count matrices were further analyzed using the R package Seurat version 3.1 (Stuart et al., 2019). Gene count measurements were normalized for each cell by library size and log-transformed using a size factor of 10,000 molecules per cell. The data was further scaled to unit variance and zero mean implemented in the “ScaleData” function. Cell types already annotated by the authors in the

original study were used and thus, no clustering was performed. Seurat's "DotPlot" function was used to generate plots shown in Figure 1B to visualize *ACE2* and *TMPRSS*2 scaled expression.

QUANTIFICATION AND STATISTICAL ANALYSIS

Statistical analysis. Bulk RNA-seq data are expressed as mean ± standard error of mean (Figures 1A). Sample size (n) is provided as the number of independent donor samples. A p-value less than 0.05 was considered significant. Statistical analysis (unpaired t-test) was performed using GraphPad Prism software.

ADDITIONAL RESOURCES

None.

Figure S1. Related to Figure 1 and 2. Testing and Characterization of Four ACE2-directed Antibodies on Human Pancreatic Tissue. (**A-E**) Characterization of ACE2 antibody (red, ab15348) used by Yang et al. (Yang et al., 2020). Mouse kidney tissue served as a positive control for ACE2 (**A**), while normal adult human pancreatic tissue incubated with anti-rabbit-Cy3 secondary antibody only served as a negative control (**B**). Normal adult human pancreas labeled for ACE2 (red), INS (green, β cells) and GCG (blue, α cells) (**C-E**). Inset area is marked by a yellow box in MERGE column. Scale bars are 100 μm (**A-E**) and 50 μm (Inset, **E**). (**F-J**) Characterization of ACE2 antibody (red, R&D MAB933) at same dilution (1:33) reported by Fignani et al. (preprint: Fignani, 2020). Human kidney tissue served as a positive control for ACE2 (**F**), while normal adult human pancreatic tissue incubated with anti-mouse-Cy3 secondary antibody only served as a negative control (**G**). Normal adult human pancreas labeled for ACE2 (red), INS (green, β cells) and GCG (blue, α cells) (**H-J**). Inset area is marked by a yellow box in MERGE column. Scale bars are 50 μm (**F-J**) and 25 μm (Inset, **J**). (**K-O**) Characterization of ACE2 antibody (red, R&D AF933) at same dilution (1:200) reported by Yang et al. (Yang et al., 2020). Human kidney served as a positive control for ACE2 (**K**), while normal adult human pancreatic tissue incubated with anti-goat-Cy3 secondary antibody only served as a negative control (**L**). Normal adult human pancreas labeled for ACE2 (red), INS (green, β cells) and GCG (blue, α cells) (**M-O**). Inset area is marked by a yellow box in MERGE column. Scale bars are 50 μm (**K-O**) and 25 μm (Inset, **O**). (**P-S**) Characterization of ACE2 antibody (red, HPA000288) used by the Human Protein Atlas (Uhlen et al., 2015) and Hikmet et al. (Hikmet et al., 2020). Human kidney tissue served as a positive control for ACE2 (**P**). Normal adult human pancreas labeled for ACE2 (red) and INS (green, β cells) (**Q-S**). Inset area is marked by a white dashed box in MERGE column. Scale bars are 100 μm (**P-S**) and 50 μm (Inset, **S**). DAPI (white). Human pancreatic donor information is available in Table S1 (**B**, donor N8; **C-E**, donor N4; **G-J**, donor N2; **L-O**, donor N7; **Q-S**, donor N8).

Figure S2. Related to Figure 2. ACE2 and TMPRSS2 Protein is Not Detected by Immunofluorescence in α or β Cells from Normal, T2D or T1D adult donors. SARS-CoV-2 cell entry markers ACE2 (antibody ab15348) and TMPRSS2, both shown in red, are not detected in islet α cells (GCG, blue) or β cells (INS, green) in pancreatic sections from adult donors without diabetes (**A-H**) or donors with type 2 (**I-N**) or type 1 (**O-V**) diabetes. Insets are depicted by a yellow box. DAPI (white). Scale bars are 100 μm (**A-V**) and 25 μm (Insets). Human islet and pancreatic donor information is available in Table S1 (**A-D**, donors N3, N7, N9, N8; **E-H**, donors N14, N12, N11, N10; **I-L**, donors 2L, 2B, 2G, 2I; **M-N**, donors 2H, 2G; **O-R**, donors 1B, 1D, 1C, 1A; **S-V**, donors 1H, 1K, 1J, 1G).

Figure S3. Related to Figure 2. DPP4 is Expressed in α cells of Adult Normal and Diabetic Donors. DPP4 (red) is expressed in human pancreatic islet α cells (GCG, blue; Merged, magenta) but not β cells (INS, green) in pancreatic sections from adult donors without diabetes (**A-C**) or donors with type 2 (**D-F**) or type 1 (**G-I**) diabetes. Scale bars are 50 μm (**A-I**). Human islet and pancreatic donor information is available in Table S1 (**A-C**, donor N8; **D-F**, donor 2K; **G-I**, donor 1H). (**J**) Dot plots of *ACE2* and *TMPRSS2* expression compared with cell type-enriched genes, including DPP4, from a previously published single cell (sc) RNA-seq datasets (Camunas-Soler et al., 2020). Dot size indicates percentage of cells in a given population expressing the gene; dot color represents scaled average expression. Dotted line highlights *ACE2* and *TMPRSS2* expression.

Figure S4. Related to Figure 3. ACE2 is Localized to Islet and Exocrine Capillaries in Adult Human Pancreas of T2D and T1D donors. Representative images of endothelial cells (CD31, white) and ACE2-positive perivascular cells (red; antibody ab15348) in islet (**A-H'**) and

exocrine tissue microvasculature (**I-P'**) of individuals with type 2 and type 1 diabetes. DAPI (white). Yellow arrowheads point to CD31-positive endothelial cells, while magenta arrowheads point to perivascular ACE2-positive cells. Insets (**A'-P'**) are depicted by yellow boxes in **A-P**. ACE2 positive perivascular cells abut extracellular matrix marker collagen-IV within the vascular basement membrane (collagen-IV [COL4], green; **D, D', H, H', L, L', P, P'**). ACE2 labeling was reduced in both islets (**E-H'**) and exocrine tissue of individuals with type 1 diabetes (**M-P'**) compared to normal donors and those with type 2 diabetes (Figure 2). Scale bars are 50 μm (**A-P**) and 10 μm (Insets, **A'-P'**). Human pancreatic donor information is available in Table S1 (**A-D'**, donor 2E; **E-H'**, donor 1F; **I-L'**, donor 2E; **M-P'**, donor 1C).

REFERENCES

Almaca, J., Weitz, J., Rodriguez-Diaz, R., Pereira, E., and Caicedo, A. (2018). The pericyte of the pancreatic islet regulates capillary diameter and local blood flow. Cell Metab *27*, 630-644 e634.
Apicella, M., Campopiano, M.C., Mantuano, M., Mazoni, L., Coppelli, A., and Del Prato, S. (2020). COVID-19 in people with diabetes: understanding the reasons for worse outcomes. Lancet Diabetes Endocrinol.
Arda, H.E., Li, L., Tsai, J., Torre, E.A., Rosli, Y., Peiris, H., Spitale, R.C., Dai, C., Gu, X., Qu, K., et al. (2016). Age-dependent pancreatic gene regulation reveals mechanisms governing human beta cell function. Cell Metab *23*, 909-920.
Ashok, A., Faghih, M., and Singh, V.K. (2020). Mild Pancreatic Enzyme Elevations in COVID-19 Pneumonia: Synonymous with Injury or Noise? Gastroenterology.
Balamurugan, A.N., Gu, Y., Miyamoto, M., Wang, W., Inoue, K., and Tabata, Y. (2003). Isolation, culture, and functional characteristics of diabetic islets [corrected]. Pancreas *26*, 102-103.
Baron, M., Veres, A., Wolock, S.L., Faust, A.L., Gaujoux, R., Vetere, A., Ryu, J.H., Wagner, B.K., Shen-Orr, S.S., Klein, A.M., et al. (2016). A single-cell transcriptomic map of the human and mouse pancreas reveals inter- and intra-cell population structure. Cell Syst *3*, 346-360 e344.
Blodgett, D.M., Nowosielska, A., Afik, S., Pechhold, S., Cura, A.J., Kennedy, N.J., Kim, S., Kucukural, A., Davis, R.J., Kent, S.C., et al. (2015). Novel observations from next-generation RNA sequencing of highly purified human adult and fetal islet cell subsets. Diabetes *64*, 3172-3181.
Bonney, G.K., Gao, Y., Chew, C.A., and Windsor, J.A. (2020). SARS-COV-2 associated acute pancreatitis: Cause, consequence or epiphenomenon? Pancreatology.
Bornstein, S.R., Rubino, F., Khunti, K., Mingrone, G., Hopkins, D., Birkenfeld, A.L., Boehm, B., Amiel, S., Holt, R.I., Skyler, J.S., et al. (2020). Practical recommendations for the management of diabetes in patients with COVID-19. Lancet Diabetes Endocrinol *8*, 546-550.
Brissova, M., Aamodt, K., Brahmachary, P., Prasad, N., Hong, J.Y., Dai, C., Mellati, M., Shostak, A., Poffenberger, G., Aramandla, R., et al. (2014). Islet microenvironment, modulated by vascular endothelial growth factor-A signaling, promotes beta cell regeneration. Cell Metab *19*, 498-511.
Brissova, M., Fowler, M.J., Nicholson, W.E., Chu, A., Hirshberg, B., Harlan, D.M., and Powers, A.C. (2005). Assessment of human pancreatic islet architecture and composition by laser scanning confocal microscopy. J Histochem Cytochem *53*, 1087-1097.
Brissova, M., Haliyur, R., Saunders, D., Shrestha, S., Dai, C., Blodgett, D.M., Bottino, R., Campbell-Thompson, M., Aramandla, R., Poffenberger, G., et al. (2018). alpha Cell Function and Gene Expression Are Compromised in Type 1 Diabetes. Cell Rep *22*, 2667-2676.
Bruno, G., Fabrizio, C., Santoro, C.R., and Buccoliero, G.B. (2020). Pancreatic injury in the course of coronavirus disease 2019: A not-so-rare occurrence. J Med Virol.
Camunas-Soler, J., Dai, X.Q., Hang, Y., Bautista, A., Lyon, J., Suzuki, K., Kim, S.K., Quake, S.R., and MacDonald, P.E. (2020). Patch-seq links single-cell transcriptomes to human islet dysfunction in diabetes. Cell Metab *31*, 1017-1031 e1014.
Cariou, B., Hadjadj, S., Wargny, M., Pichelin, M., Al-Salameh, A., Allix, I., Amadou, C., Arnault, G., Baudoux, F., Bauduceau, B., et al. (2020). Phenotypic characteristics and prognosis of inpatients with COVID-19 and diabetes: the CORONADO study. Diabetologia *63*, 1500-1515.

Chee, Y.J., Ng, S.J.H., and Yeoh, E. (2020). Diabetic ketoacidosis precipitated by Covid-19 in a patient with newly diagnosed diabetes mellitus. Diabetes Res Clin Pract *164*, 108166.
Chen, L., Li, X., Chen, M., Feng, Y., and Xiong, C. (2020). The ACE2 expression in human heart indicates new potential mechanism of heart injury among patients infected with SARS-CoV-2. Cardiovasc Res *116*, 1097-1100.
Dai, C., Hang, Y., Shostak, A., Poffenberger, G., Hart, N., Prasad, N., Phillips, N., Levy, S.E., Greiner, D.L., Shultz, L.D., et al. (2017). Age-dependent human beta cell proliferation induced by glucagon-like peptide 1 and calcineurin signaling. J Clin Invest *127*, 3835-3844.
Drucker, D.J. (2020). Coronavirus Infections and Type 2 Diabetes-Shared Pathways with Therapeutic Implications. Endocr Rev *41*.
Filippi, C.M., and von Herrath, M.G. (2008). Viral trigger for type 1 diabetes: pros and cons. Diabetes *57*, 2863-2871.
Goldman, N., Fink, D., Cai, J., Lee, Y.N., and Davies, Z. (2020). High prevalence of COVID-19-associated diabetic ketoacidosis in UK secondary care. Diabetes Res Clin Pract *166*, 108291.
Gupta, A., Madhavan, M.V., Sehgal, K., Nair, N., Mahajan, S., Sehrawat, T.S., Bikdeli, B., Ahluwalia, N., Ausiello, J.C., Wan, E.Y., et al. (2020). Extrapulmonary manifestations of COVID-19. Nat Med *26*, 1017-1032.
Hamming, I., Timens, W., Bulthuis, M.L., Lely, A.T., Navis, G., and van Goor, H. (2004). Tissue distribution of ACE2 protein, the functional receptor for SARS coronavirus. A first step in understanding SARS pathogenesis. J Pathol *203*, 631-637.
He, L., Mae, M., Sun, Y., Muhl, L, Nahar, K., et al (2020). Pericyte-specific vascular expression of SARS-CoV-2 receptor ACE2 – implications for microvascular inflammation and hypercoagulopathy in COVID-19 patients. Biorxiv.
Heaney, A.I., Griffin, G.D., and Simon, E.L. (2020). Newly diagnosed diabetes and diabetic ketoacidosis precipitated by COVID-19 infection. Am J Emerg Med.
Hikmet, F., Mear, L., Edvinsson, A., Micke, P., Uhlen, M., and Lindskog, C. (2020). The protein expression profile of ACE2 in human tissues. Mol Syst Biol *16*, e9610.
Hoffmann, M., Kleine-Weber, H., Schroeder, S., Kruger, N., Herrler, T., Erichsen, S., Schiergens, T.S., Herrler, G., Wu, N.H., Nitsche, A., et al. (2020). SARS-CoV-2 Cell Entry Depends on ACE2 and TMPRSS2 and Is Blocked by a Clinically Proven Protease Inhibitor. Cell *181*, 271-280 e278.
Kaestner, K.H., Powers, A.C., Naji, A., Consortium, H., and Atkinson, M.A. (2019). NIH Initiative to Improve Understanding of the Pancreas, Islet, and Autoimmunity in Type 1 Diabetes: The Human Pancreas Analysis Program (HPAP). Diabetes *68*, 1394-1402.
Karimzadeh, S., Manzuri, A., Ebrahimi, M., and Huy, N.T. (2020). COVID-19 presenting as acute pancreatitis: Lessons from a patient in Iran. Pancreatology.
Kim, N.Y., Ha, E., Moon, J.S., Lee, Y.H., and Choi, E.Y. (2020). Acute Hyperglycemic Crises with Coronavirus Disease-19: Case Reports. Diabetes Metab J *44*, 349-353.
Lan, J., Ge, J., Yu, J., Shan, S., Zhou, H., Fan, S., Zhang, Q., Shi, X., Wang, Q., Zhang, L., et al. (2020). Structure of the SARS-CoV-2 spike receptor-binding domain bound to the ACE2 receptor. Nature *581*, 215-220.
Li, J., Wang, X., Chen, J., Zuo, X., Zhang, H., and Deng, A. (2020a). COVID-19 infection may cause ketosis and ketoacidosis. Diabetes Obes Metab.
Li, Y., Zhang, Z., Yang, L., Lian, X., Xie, Y., Li, S., Xin, S., Cao, P., and Lu, J. (2020b). The MERS-CoV Receptor DPP4 as a Candidate Binding Target of the SARS-CoV-2 Spike. iScience *23*, 101160.

Meireles, P.A., Bessa, F., Gaspar, P., Parreira, I., Silva, V.D., Mota, C., and Alvoeiro, L. (2020). Acalculous acute pancreatitis in a COVID-19 patient. Eur J Case Rep Intern Med *7*, 001710.
Nair, G.G., Liu, J.S., Russ, H.A., Tran, S., Saxton, M.S., Chen, R., Juang, C., Li, M.L., Nguyen, V.Q., Giacometti, S., et al. (2019). Recapitulating endocrine cell clustering in culture promotes maturation of human stem-cell-derived beta cells. Nat Cell Biol *21*, 263-274.
preprint: Fignani, D., Licata, G., Brusco, N., Nigi, L., Grieco, G., Marselli, L., Overbergh, L., Gysemans, C., Colli, M., Marchetti, P., Mathieu, C., Eizirik, D., Sebastiani, G., Dotta, F. (2020). SARS-CoV-2 receptor angiotensin I-converting enzyme type 2 is expressed in human pancreatic islet β-cells and is upregulated by inflammatory stress. BioRxiv.
Rabice, S.R., Altshuler, P.C., Bovet, C., Sullivan, C., and Gagnon, A.J. (2020). COVID-19 infection presenting as pancreatitis in a pregnant woman: A case report. Case Rep Womens Health *27*, e00228.
Rafique, S., and Ahmed, F.W. (2020). A Case of Combined Diabetic Ketoacidosis and Hyperosmolar Hyperglycemic State in a Patient With COVID-19. Cureus *12*, e8965.
Riddle, M.C., Buse, J.B., Franks, P.W., Knowler, W.C., Ratner, R.E., Selvin, E., Wexler, D.J., and Kahn, S.E. (2020). COVID-19 in People With Diabetes: Urgently Needed Lessons From Early Reports. Diabetes Care *43*, 1378-1381.
Sanders, J.M., Monogue, M.L., Jodlowski, T.Z., and Cutrell, J.B. (2020). Pharmacologic Treatments for Coronavirus Disease 2019 (COVID-19): A Review. JAMA.
Segerstolpe, A., Palasantza, A., Eliasson, P., Andersson, E.M., Andreasson, A.C., Sun, X., Picelli, S., Sabirsh, A., Clausen, M., Bjursell, M.K., et al. (2016). Single-cell transcriptome profiling of human pancreatic islets in health and type 2 diabetes. Cell Metab *24*, 593-607.
Shang, J., Wan, Y., Luo, C., Ye, G., Geng, Q., Auerbach, A., and Li, F. (2020). Cell entry mechanisms of SARS-CoV-2. Proc Natl Acad Sci U S A *117*, 11727-11734.
Stuart, T., Butler, A., Hoffman, P., Hafemeister, C., Papalexi, E., Mauck, W.M., 3rd, Hao, Y., Stoeckius, M., Smibert, P., and Satija, R. (2019). Comprehensive Integration of Single-Cell Data. Cell *177*, 1888-1902 e1821.
Vankadari, N., and Wilce, J.A. (2020). Emerging WuHan (COVID-19) coronavirus: glycan shield and structure prediction of spike glycoprotein and its interaction with human CD26. Emerg Microbes Infect *9*, 601-604.
Wang, F., Wang, H., Fan, J., Zhang, Y., Wang, H., and Zhao, Q. (2020). Pancreatic Injury Patterns in Patients With Coronavirus Disease 19 Pneumonia. Gastroenterology *159*, 367-370.
Wang, S., Ma, P., Zhang, S., et al (2020). Fasting blood glucose at admission is an independent predictor for 28-day mortality in patients with COVID-19 without previous diagnosis of diabetes: a multi-centre retrospective study. Diabetologia.
Wiersinga, W.J., Rhodes, A., Cheng, A.C., Peacock, S.J., and Prescott, H.C. (2020). Pathophysiology, Transmission, Diagnosis, and Treatment of Coronavirus Disease 2019 (COVID-19): A Review. JAMA.
Wright, J.J., Saunders, D.C., Dai, C., Poffenberger, G., Cairns, B., Serreze, D.V., Harlan, D.M., Bottino, R., Brissova, M., and Powers, A.C. (2020). Decreased pancreatic acinar cell number in type 1 diabetes. Diabetologia *63*, 1418-1423.
Yang, J.K., Lin, S.S., Ji, X.J., and Guo, L.M. (2010). Binding of SARS coronavirus to its receptor damages islets and causes acute diabetes. Acta Diabetol *47*, 193-199.

Yang, L., Han, Y., Nilsson-Payant, B.E., Gupta, V., Wang, P., Duan, X., Tang, X., Zhu, J., Zhao, Z., Jaffre, F., et al. (2020). A human pluripotent stem cell-based platform to study SARS-CoV-2 tropism and model virus infection in human cells and organoids. Cell Stem Cell *27*, 125-136 e127.
Zhu, L., She, Z.G., Cheng, X., Qin, J.J., Zhang, X.J., Cai, J., Lei, F., Wang, H., Xie, J., Wang, W., et al. (2020). Association of Blood Glucose Control and Outcomes in Patients with COVID-19 and Pre-existing Type 2 Diabetes. Cell Metab *31*, 1068-1077 e1063.

Figure 1

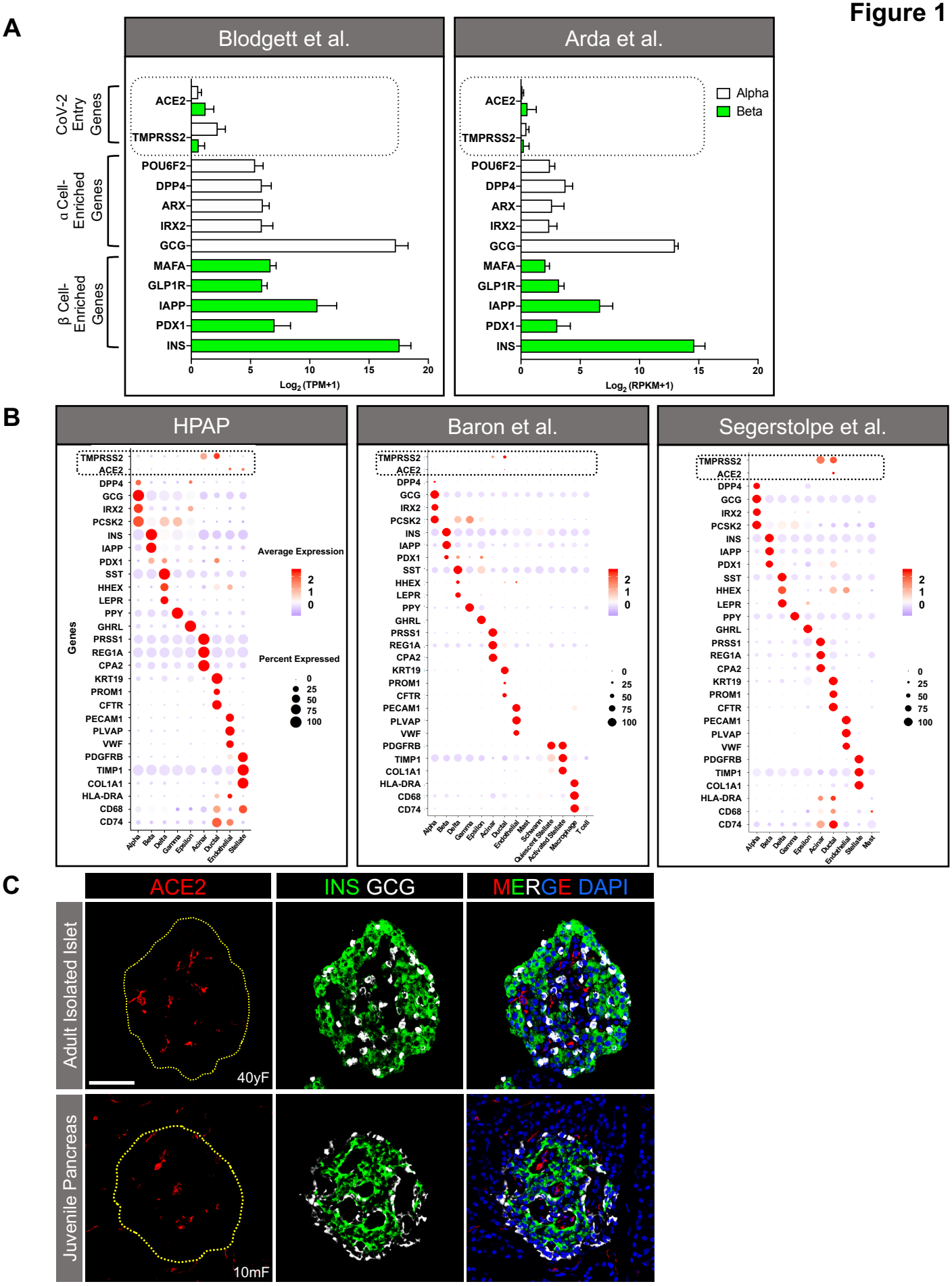
A
Blodgett et al.
Arda et al.
CoV-2 Entry Genes
α Cell-Enriched Genes
β Cell-Enriched Genes
ACE2
TMPRSS2
POU6F2
DPP4
ARX
IRX2
GCG
MAFA
GLP1R
IAPP
PDX1
INS
Alpha
Beta
Log2 (TPM+1)
Log2 (RPKM+1)
B
HPAP
Baron et al.
Segerstolpe et al.
Genes
Average Expression
Percent Expressed
Alpha
Beta
Delta
Gamma
Epsilon
Acinar
Ductal
Endothelial
Stellate
Mast
Schwann
Quiescent Stellate
Activated Stellate
Macrophage
T cell
C
ACE2
INS GCG
MERGE DAPI
Adult Isolated Islet
Juvenile Pancreas
40yF
10mF

Figure 2

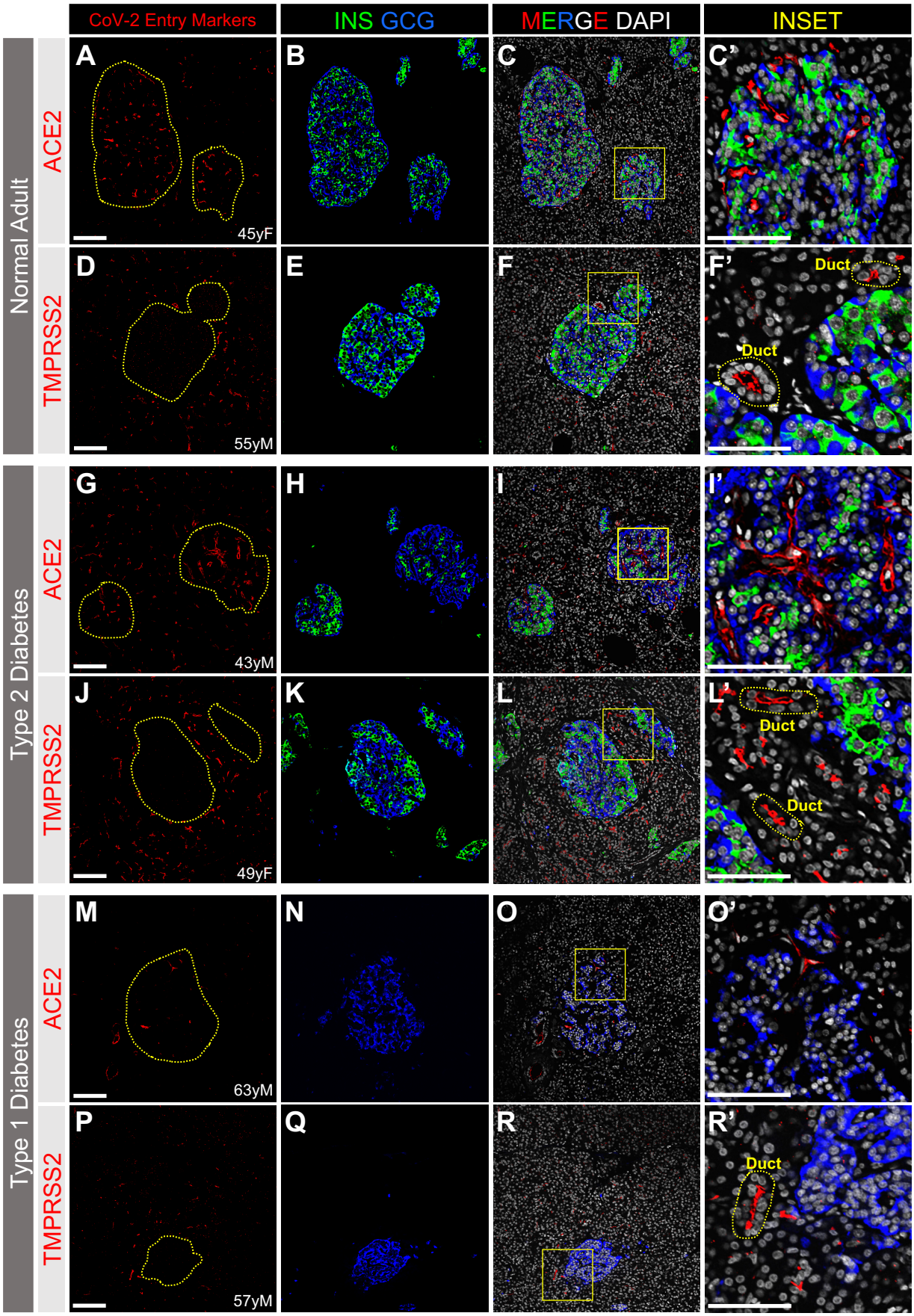
CoV-2 Entry Markers
INS GCG
MERGE DAPI
INSET
Normal Adult
ACE2
TMPRSS2
Type 2 Diabetes
Type 1 Diabetes
A
B
C
C'
D
E
F
F'
G
H
I
I'
J
K
L
L'
M
N
O
O'
P
Q
R
R'
45yF
55yM
43yM
49yF
63yM
57yM
Duct

Figure 3

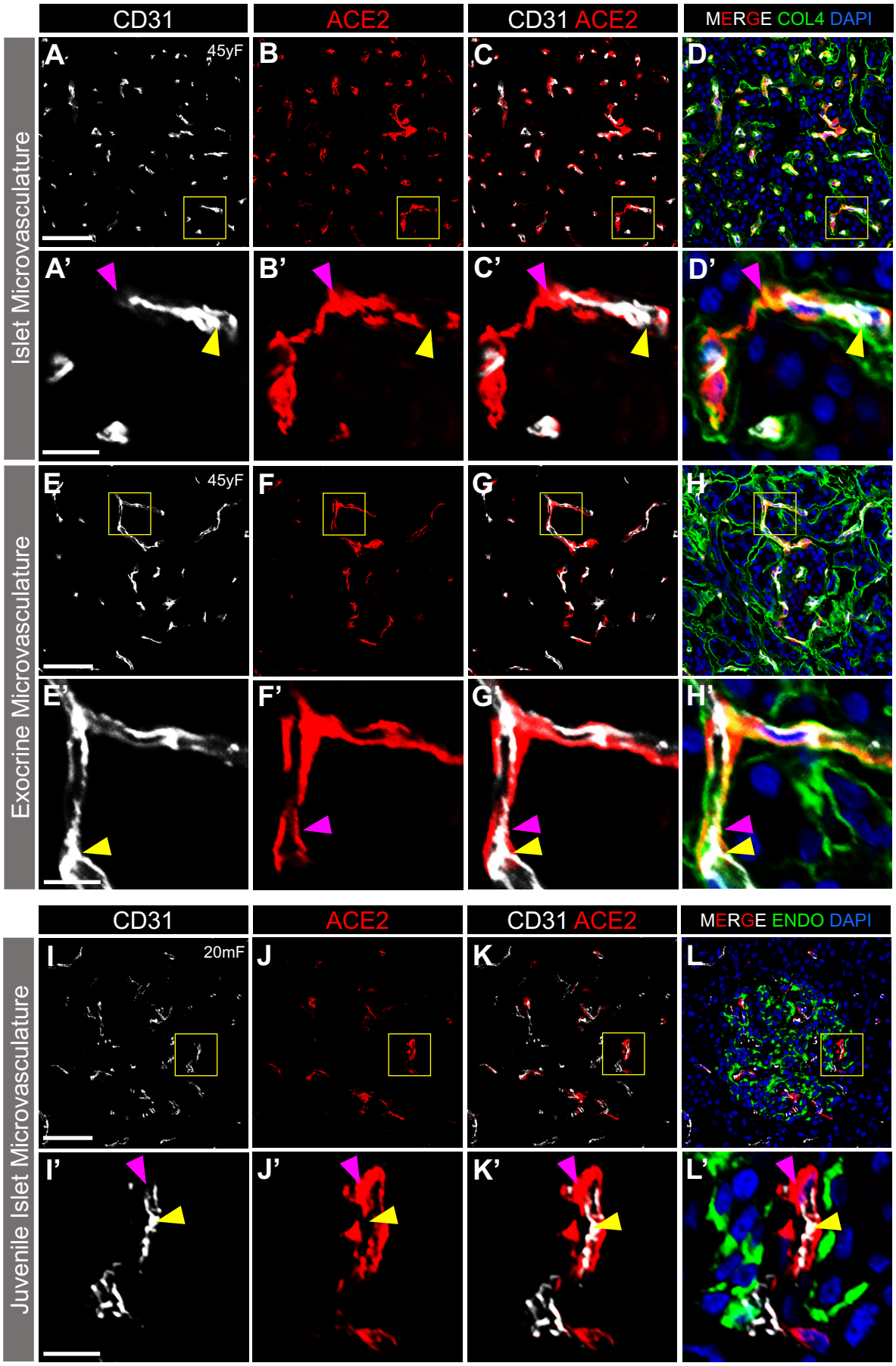
CD31
ACE2
CD31 ACE2
MERGE COL4 DAPI
Islet Microvasculature
A
45yF
B
C
D
A'
B'
C'
D'
Exocrine Microvasculature
E
45yF
F
G
H
E'
F'
G'
H'
CD31
ACE2
CD31 ACE2
MERGE ENDO DAPI
Juvenile Islet Microvasculature
I
20mF
J
K
L
I'
J'
K'
L'

Figure 4

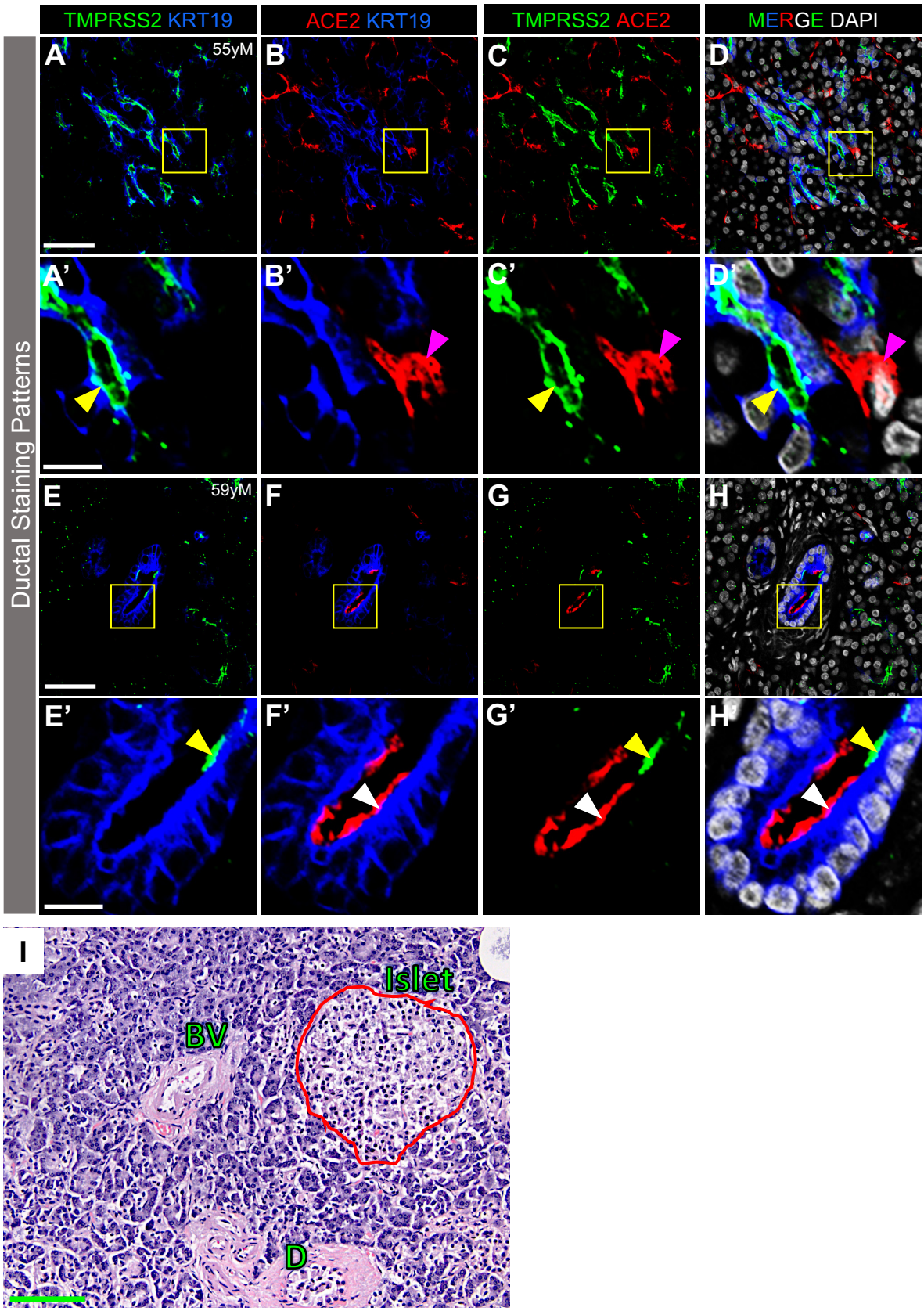
TMPRSS2 KRT19
ACE2 KRT19
TMPRSS2 ACE2
MERGE DAPI
Ductal Staining Patterns
A
55yM
B
C
D
A'
B'
C'
D'
E
59yM
F
G
H
E'
F'
G'
H'
I
Islet
BV
D

Figure S1

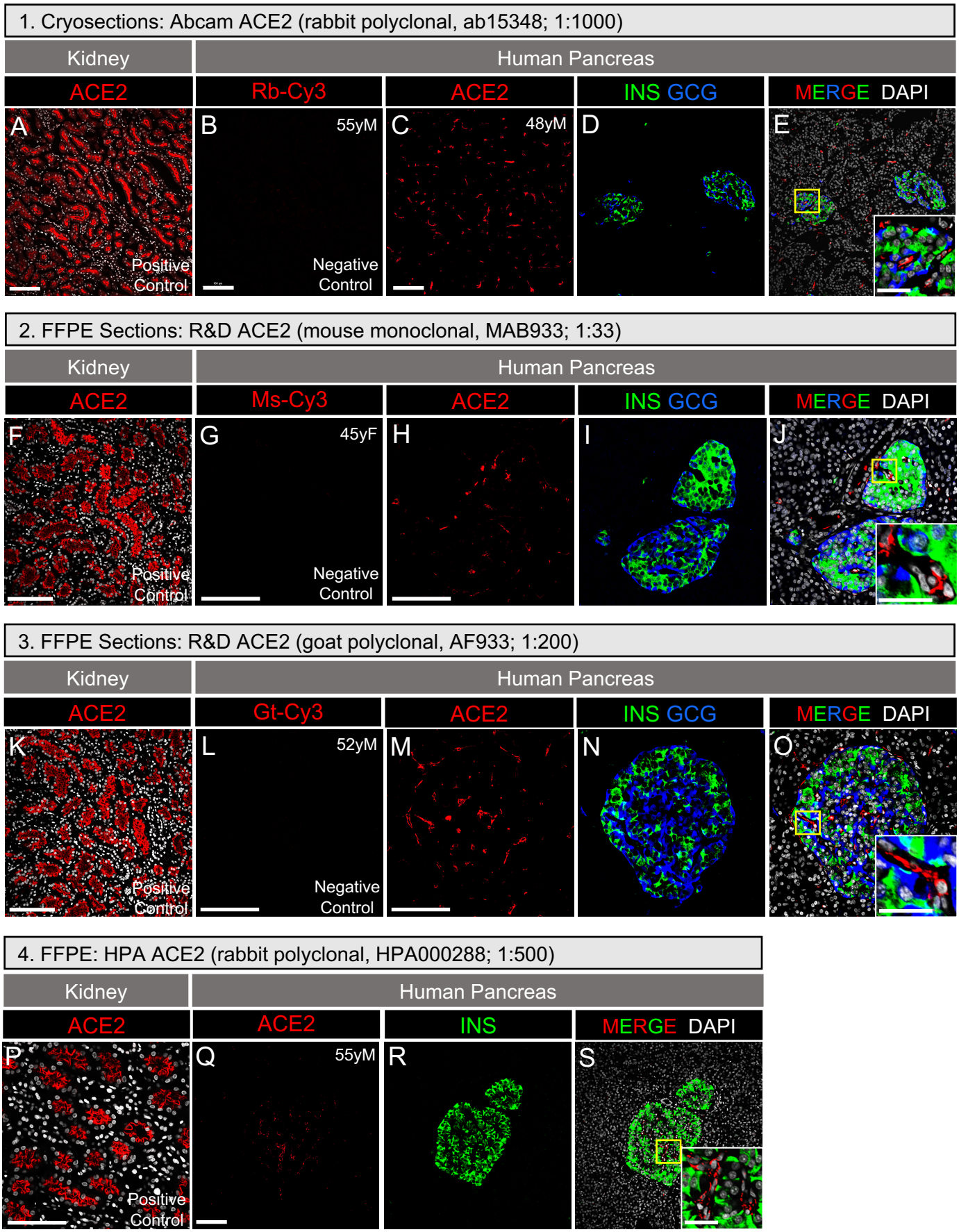
1. Cryosections: Abcam ACE2 (rabbit polyclonal, ab15348; 1:1000)
Kidney
Human Pancreas
ACE2
Rb-Cy3
ACE2
INS GCG
MERGE DAPI
A
Positive Control
B
55yM
Negative Control
C
48yM
D
E
2. FFPE Sections: R&D ACE2 (mouse monoclonal, MAB933; 1:33)
Kidney
Human Pancreas
ACE2
Ms-Cy3
ACE2
INS GCG
MERGE DAPI
F
Positive Control
G
45yF
Negative Control
H
I
J
3. FFPE Sections: R&D ACE2 (goat polyclonal, AF933; 1:200)
Kidney
Human Pancreas
ACE2
Gt-Cy3
ACE2
INS GCG
MERGE DAPI
K
Positive Control
L
52yM
Negative Control
M
N
O
4. FFPE: HPA ACE2 (rabbit polyclonal, HPA000288; 1:500)
Kidney
Human Pancreas
ACE2
ACE2
INS
MERGE DAPI
P
Positive Control
Q
55yM
R
S

Figure S2

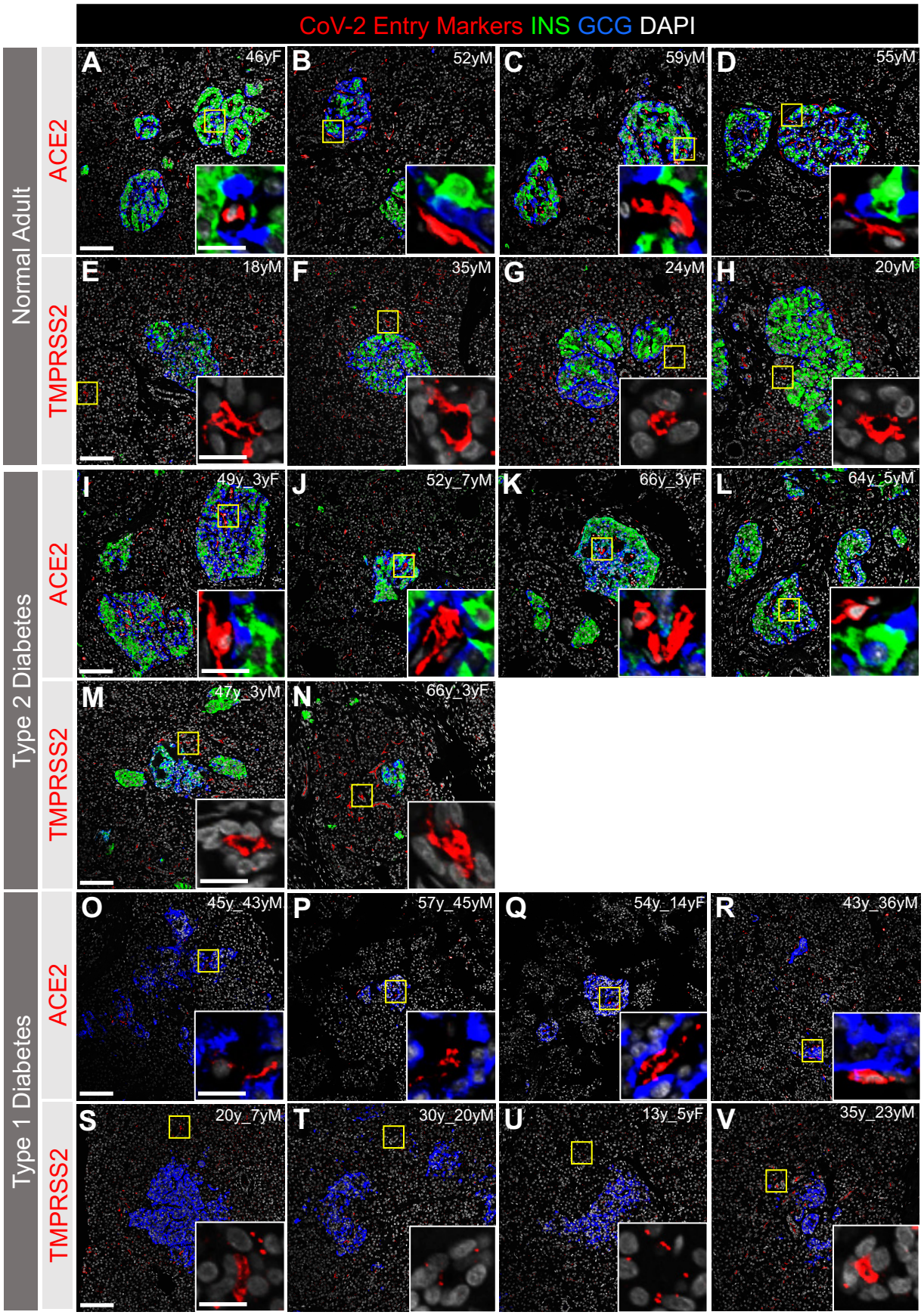
CoV-2 Entry Markers INS GCG DAPI
Normal Adult
ACE2
TMPRSS2
Type 2 Diabetes
ACE2
TMPRSS2
Type 1 Diabetes
ACE2
TMPRSS2
A 46yF
B 52yM
C 59yM
D 55yM
E 18yM
F 35yM
G 24yM
H 20yM
I 49y_3yF
J 52y_7yM
K 66y_3yF
L 64y_5yM
M 47y_3yM
N 66y_3yF
O 45y_43yM
P 57y_45yM
Q 54y_14yF
R 43y_36yM
S 20y_7yM
T 30y_20yM
U 13y_5yF
V 35y_23yM

Figure S3

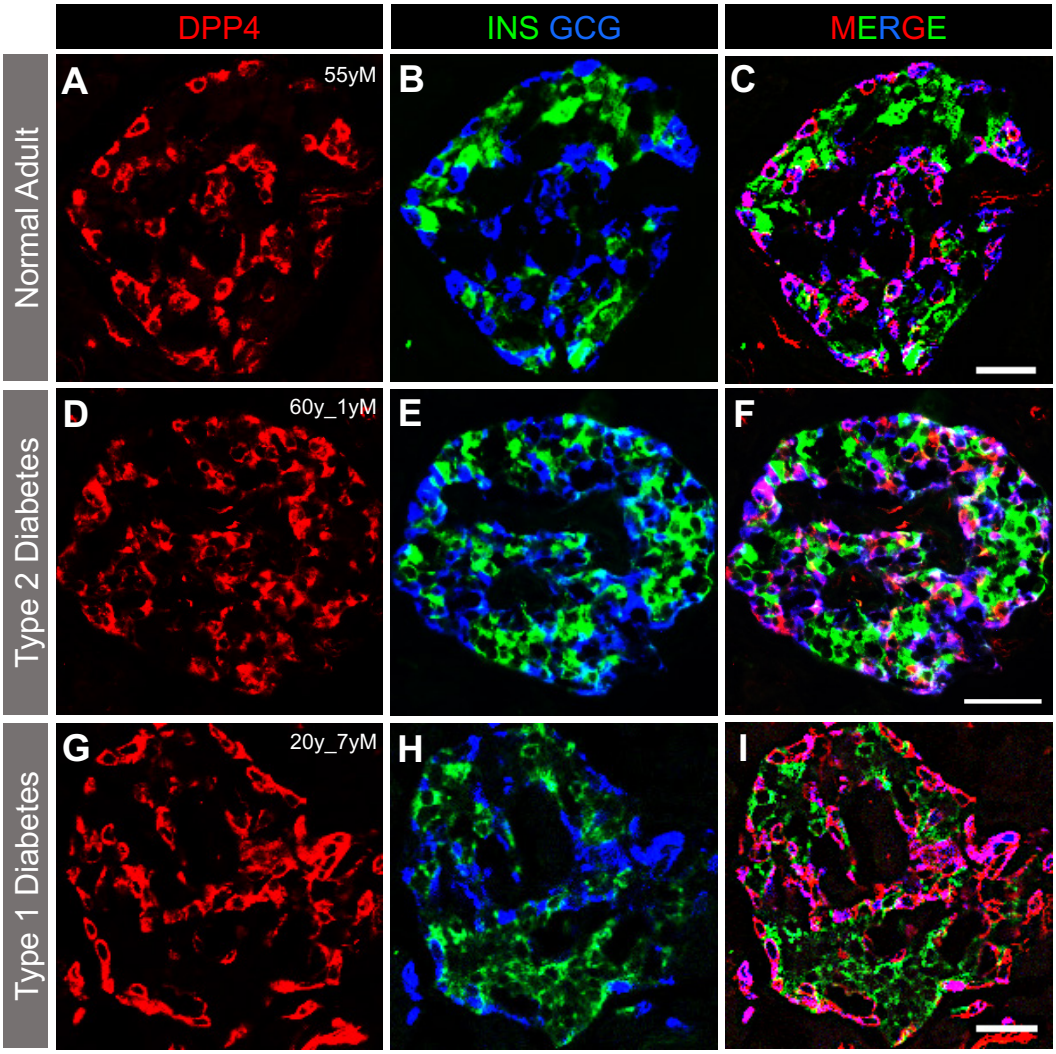
DPP4
INS GCG
MERGE
Normal Adult
Type 2 Diabetes
Type 1 Diabetes
A
55yM
B
C
D
60y_1yM
E
F
G
20y_7yM
H
I

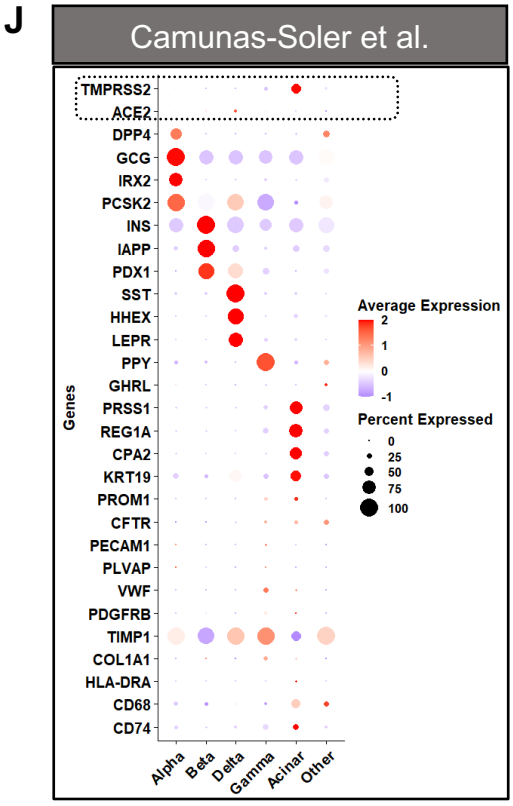
J
Camunas-Soler et al.
TMPRSS2
ACE2
DPP4
GCG
IRX2
PCSK2
INS
IAPP
PDX1
SST
HHEX
LEPR
PPY
GHRL
PRSS1
REG1A
CPA2
KRT19
PROM1
CFTR
PECAM1
PLVAP
VWF
PDGFRB
TIMP1
COL1A1
HLA-DRA
CD68
CD74
Genes
Alpha
Beta
Delta
Gamma
Acinar
Other
Average Expression
2
1
0
-1
Percent Expressed
0
25
50
75
100

Figure S4

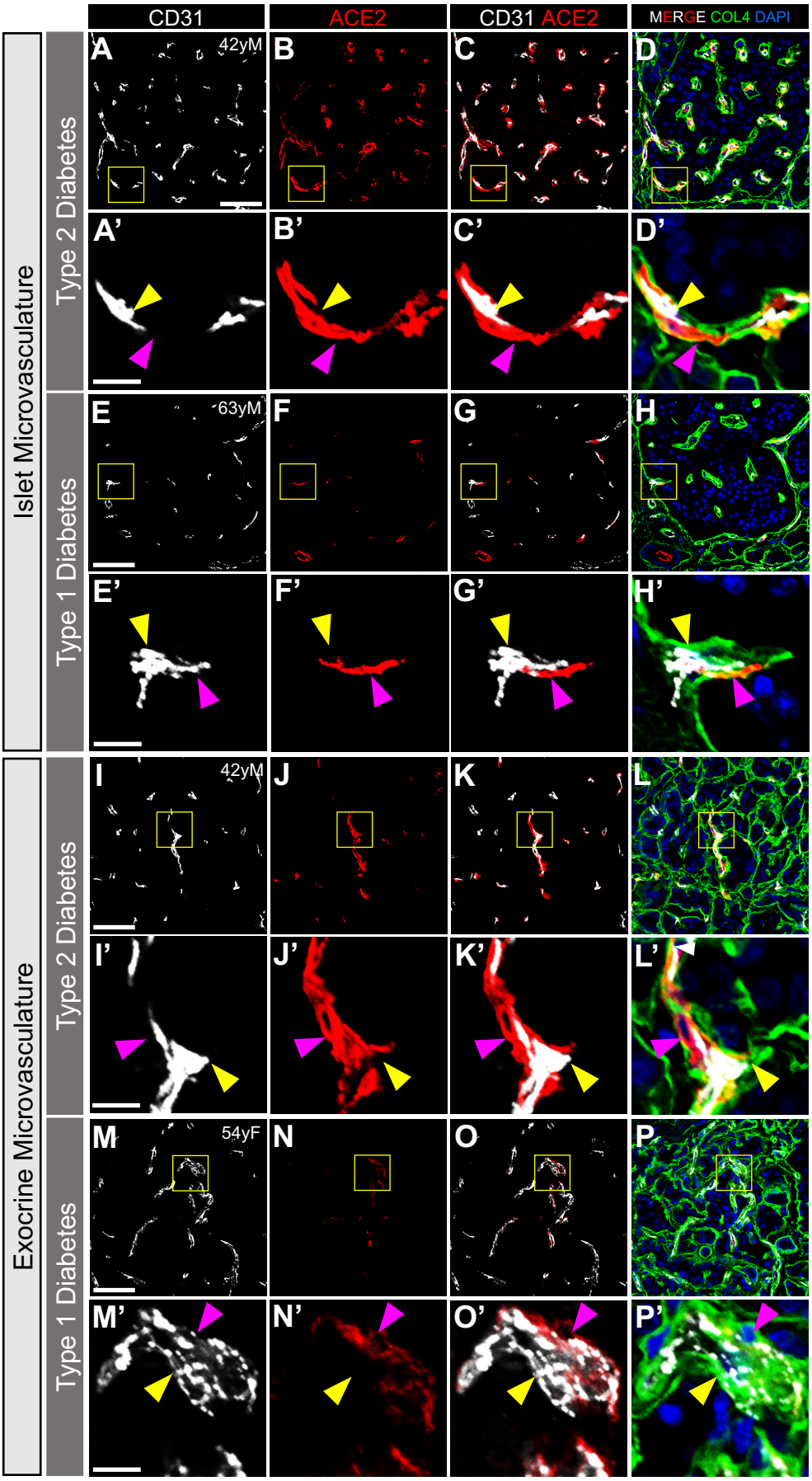
CD31
ACE2
CD31 ACE2
MERGE COL4 DAPI
Islet Microvasculature
Exocrine Microvasculature
Type 2 Diabetes
Type 1 Diabetes
Type 2 Diabetes
Type 1 Diabetes
42yM
63yM
42yM
54yF
A
B
C
D
A'
B'
C'
D'
E
F
G
H
E'
F'
G'
H'
I
J
K
L
I'
J'
K'
L'
M
N
O
P
M'
N'
O'
P'

Table S1: Related to STAR Methods. Demographic information of donors.

Donor ID		Age	Ethnicity / Race	Diabetes Duration	Sex	BMI	Cause of Death	Tissue/Islet Source
Juvenile (Histology)	J1	5 days	Caucasian	--	F	14.9	Anoxia	IIAM
	J2	3 months	Caucasian	--	M	16.8	Anoxia	NDRI
	J3	10 months	Caucasian	--	F	15.4	CVA	NDRI
	J4	20 months	Caucasian	--	F	23.5	Anoxia	IIAM
	J5	5 years	Caucasian	--	M	16.2	Anoxia	IIAM
Normal Adult (Histology)	N1	42 years	Caucasian	--	M	32.2	Overdose	TNDS
	N2	45 years	Caucasian	--	F	29.7	Anoxia	OPO
	N3	46 years	Caucasian	--	F	32.9	CVA	IIAM
	N4	48 years	Caucasian	--	M	24.6	Anoxia	OPO
	N5	51 years	Caucasian	--	M	20.4	Anoxia	OPO
	N6	52 years	Black	--	M	29.2	ICH	TNDS
	N7	52 years	Caucasian	--	M	28.1	Head Trauma	OPO
	N8	55 years	Black	--	M	35.6	CVA	IIAM
	N9	59 years	Caucasian	--	M	32.7	Head Trauma	IIAM
	N10	20 years	Hispanic	--	M	19.4	Head Trauma	IIAM
	N11	24 years	Caucasian	--	M	35.5	ICH	IIAM
	N12	35 years	Caucasian	--	M	26.8	Head Trauma	IIAM
	N13	20 years	Caucasian	--	M	27.8	Head Trauma	NDRI
	N14	18 years	Caucasian	--	M	25.1	Head Trauma	IIAM
Adult T1D (Histology)	1A	43 years	N/A	36 years	M	31.2	CVA	NDRI
	1B	45 years	Caucasian	43 years	M	25.0	Anoxia	IIAM
	1C	54 years	Caucasian	14 years	F	24.9	Anoxia	IIAM
	1D	57 years	Black	45 years	M	33.3	CVA	IIAM
	1E	58 years	Caucasian	31 years	M	21.8	Anoxia	NDRI
	1F	63 years	Caucasian	44 years	M	24.1	Anoxia	IIAM
	1G	35 years	Caucasian	23 years	M	26.9	Anoxia	NDRI
	1H	20 years	Caucasian	7 years	M	25.5	Anoxia	NDRI
	1I	27 years	Caucasian	17 years	M	18.4	Anoxia	NDRI
	1J	13 years	Caucasian	5 years	M	19.1	Anoxia	IIAM
	1K	30 years	Caucasian	20 years	M	29.8	Anoxia	NDRI
Adult T2D (Histology)	2A	44 years	Caucasian	7 years	M	44.4	CVA	IIAM
	2B	52 years	Caucasian	7 years	M	33.6	CVA	IIAM
	2C	52 years	Asian	10 years	F	21.9	CVA	NDRI
	2D	52 years	Caucasian	< 1 year	F	29.2	CVA	IIAM
	2E	42 years	Black	< 1 year	M	42.0	CVA	IIAM
	2F	43 years	Black	1 year	M	36.0	Head Trauma	IIAM
	2G	66 years	Caucasian	3 years	F	32.8	CVA	IIAM
	2H	47 years	Caucasian	3 years	M	31.3	CVA	IIAM
	2I	64 years	Caucasian	5 years	M	33.2	ICH	IIAM
	2J	59 years	Caucasian	6 years	F	27.5	CVA	IIAM
	2K	60 years	Caucasian	1 year	M	38.3	CVA	IIAM
	2L	49 years	Caucasian	3 years	F	33.8	CVA	IIAM
Normal Adult Islets	I1	40 years	Caucasian	--	F	30.8	Head Trauma	IIDP
	I2	41 years	N/A	--	M	20.3	N/A	IIDP
	I3	42 years	Caucasian	--	M	32.2	Overdose	IIDP

(Gels and scRNA-Seq)	HPAP022	39 years	Caucasian	--	F	34.7	Anoxia	HPAP
	HPAP026	24 years	Caucasian	--	M	20.8	Anoxia	HPAP
	HPAP034	13 years	Caucasian	--	M	18.6	Head Trauma	HPAP
	HPAP035	35 years	Caucasian	--	M	26.9	Anoxia	HPAP
	HPAP036	23 years	Caucasian	--	F	16	Head Trauma	HPAP
	HPAP037	35 years	Caucasian	--	F	21.9	CVA	HPAP
	HPAP039	5 years	Caucasian	--	F	16.3	Anoxia	HPAP
	HPAP040	35 years	Caucasian	--	M	23.9	CVA	HPAP
	HPAP042	1 year	Caucasian	--	M	17.9	Anoxia	HPAP
	HPAP044	3 years	Caucasian	--	F	12	Anoxia	HPAP
	HPAP047	8 years	Caucasian	--	M	16.8	CVA	HPAP
COVID-19 Patient Autopsy Samples (Histology)	1	82 years	Caucasian	--	M	26.8	ALI	VUMC Autopsy
	2	97 years	Caucasian	--	F	19.7	ALI	VUMC Autopsy
	3	81 years	Caucasian	unknown	M	23.3	ALI	VUMC Autopsy
	4	60 years	Hispanic	--	M	36.7	ALI	VUMC Autopsy
	5	51 years	Hispanic	unknown	M	29.4	ALI	VUMC Autopsy
	6	60 years	Caucasian	--	F	38.4	PE	VUMC Autopsy
	7	71 years	Black	unknown	M	31.5	ALI	VUMC Autopsy

ALI – acute lung injury; CVA, cerebrovascular accident; HPAP – Human Pancreas Analysis Program (Human Islet Research Network); ICH, intracerebral hemorrhage; IIAM – International Institute for the Advancement of Medicine; IIDP – Integrated Islet Distribution Program; N/A – not available; NDRI – National Disease Research Interchange; OPO – Organ Procurement Organization; PE – pulmonary embolism; T1D = type 1 diabetes; T2D – type 2 diabetes; TNDS – Tennessee Donor Services, Nashville; VUMC Autopsy – Vanderbilt University Medical Center Autopsy Pathology

KEY RESOURCES TABLE

REAGENT or RESOURCE	SOURCE	IDENTIFIER
Antibodies		
Mouse anti-Cytokeratin 19 (1:1000)	Abcam	Cat# ab194399
Rabbit anti-TMPRSS2 (1:400)	Sigma	Cat# HPA035787, RRID:AB_2674782
Mouse anti-Glucagon (1:500-1:1000)	Abcam	Cat# ab10988, RRID:AB_297642
Guinea pig anti-Glucagon (1:500)	LSBio	Cat# LS-C202759-50
Rat anti-C-peptide (1:1000)	DSHB	Cat# GN-ID4, RRID:AB_2255626
Guinea pig anti-Insulin (1:500-1:1000)	Dako	Cat# A0564, RRID:AB_2617169
Rabbit anti-ACE2 (1:500)	Atlas Antibodies	Cat# HPA000288, RRID:AB_1078160
Rabbit anti-ACE2 (1:1000)	Abcam	Cat# ab15348, RRID:AB_301861
Goat anti-ACE2 (1:200, Figure S1,3A-E; 1:400, Figure 4)	R&D	Cat# AF933, RRID:AB_355722
Mouse anti-ACE2 (1:33)	R&D	Cat# MAB933, RRID:AB_2223153
Mouse anti-CD31 (1:50)	BD Biosciences	Cat# 550389, RRID:AB_2252087
Goat anti-collagen IV alpha 1 (1:500)	Novus	Cat# NBP1-26549, RRID:AB_1853202
Goat anti-DPP4 (1:200)	R&D	Cat# AF1180, RRID:AB_354651
Donkey anti-mouse-Cy2 (1:500)	Jackson ImmunoResearch	Cat# 715-225-150, RRID:AB_2340826
Donkey anti-mouse-Cy3 (1:500)	Jackson ImmunoResearch	Cat# 715-165-150, RRID:AB_2340813
Donkey anti-mouse-Cy5 (1:250 – 1:500)	Jackson ImmunoResearch	Cat# 715-175-151, RRID:AB_2340820
Donkey anti-rabbit-Cy3 (1:500)	Jackson ImmunoResearch	Cat# 711-165-152, RRID:AB_2307443
Donkey anti-rat-Cy2 (1:500)	Jackson ImmunoResearch	Cat# 712-225-153, RRID:AB_2340674
Donkey anti-guinea pig-Cy2 (1:500)	Jackson ImmunoResearch	Cat# 706-225-148, RRID:AB_2340467
Donkey anti-goat-Cy2 (1:500)	Jackson ImmunoResearch	Cat# 705-225-147, RRID:AB_2307341
Donkey anti-goat-Cy3 (1:500)	Jackson ImmunoResearch	Cat# 705-165-147, RRID:AB_2307351
Donkey anti-guinea pig-Cy5 (1:250-1:500)	Jackson ImmunoResearch	Cat# 706-175-148, RRID:AB_2340462
Normal Donkey Serum	Jackson ImmunoResearch	Cat# 017-000-121, RRID: AB_2337258
Bacterial and Virus Strains		
n/a		
Biological Samples		
Human pancreatic islets	Integrated Islet Distribution Program (IIDP)	http://iidp.coh.org, RRID: SCR_014387
Human pancreatic tissue	International Institute for the Advancement of Medicine (IIAM)	http://www.iiam.org, RRID: SCR_016172
Human pancreatic tissue	National Disease Research Interchange (NDRI)	http://ndriresource.org, RRID: SCR_000550

Chemicals, Peptides, and Recombinant Proteins		
Propidium Iodide	BD Biosciences	Cat# 556463
Antigen Unmasking Solution, Citrate-Based	Vector Laboratories	Cat# H-3300-250
1X PBS	Corning	Cat# 46-013-CM
Triton X-100	USB	Cat# 22686
BSA	Sigma	Cat# A6003-25G
Critical Commercial Assays		
RNAqueous-Micro Kit	Fisher Scientific (Invitrogen)	Cat# AM1931
High Capacity cDNA Reverse Transcription Kit	Fisher Scientific (Invitrogen)	Cat# 4368814
Deposited Data		
RNA-seq data for FACS purified human alpha and beta cells (Blodgett et al., 2015)	NCBI Gene Expression Omnibus	GEO: GSE67543
RNA-seq data for FACS purified human alpha and beta cells (Arda et al., 2016)	NCBI Gene Expression Omnibus	GEO: GSE57973
Single-cell RNA-seq data for human islets (Baron et al., 2016)	NCBI Gene Expression Omnibus	GEO: GSE84133
Single-cell RNA-seq data for human islets (Camunas-Soler et al., 2020)	NCBI Gene Expression Omnibus	GEO: GSE124742
Single-cell RNA-seq data for human islets (Segerstolpe et al., 2016)	ArrayExpress	E-MTAB-5061
Single-cell RNA-seq data for human islets (Human Pancreas Analysis Program [HPAP])	HPAP Database	https://hpap.pmacs.upenn.edu RRID:SCR_014393
Experimental Models: Cell Lines		
n/a		
Experimental Models: Organisms/Strains		
n/a		
Recombinant DNA		
n/a		
Software and Algorithms		
FV31S-SW Viewer 2.4.1.198	Olympus	https://www.olympus-lifescience.com/en/support/downloads/
Seurat 3.1 R package	(Butler et al., 2018) (Stuart et al., 2019)	N/A
Prism for macOS v.8.4.3	Graphpad Software	http://www.graphpad.com, RRID: SCR_002798

Butler, A., Hoffman, P., Smibert, P., Papalexi, E., and Satija, R. (2018). Integrating single-cell transcriptomic data across different conditions, technologies, and species. Nat Biotechnol *36*, 411-420.
Stuart, T., Butler, A., Hoffman, P., Hafemeister, C., Papalexi, E., Mauck, W.M., 3rd, Hao, Y., Stoeckius, M., Smibert, P., and Satija, R. (2019). Comprehensive Integration of Single-Cell Data. Cell *177*, 1888-1902 e1821.